

SUPPLEMENTAL MATERIAL

Experimental evidences for static charge density waves in iron oxy-pnictides

S.1: Synchrotron powder diffraction

The structural properties of $\text{La}(\text{Fe}_{1-x}\text{Mn}_x)\text{AsO}$ samples ($x = 0.02$ and 0.04) were investigated by means of high-resolution synchrotron X-ray powder diffraction analysis between 290 K and 10 K; X-ray scattering data were collected at the ID22 high-resolution powder diffraction beamline of the European Synchrotron Radiation Facility (ESRF) in Grenoble, France. Structural data at 290 K and 10 K obtained after Rietveld refinement are listed in Tables S1 and S2.

Table S1: Structural data at 290 K obtained for $\text{La}(\text{Fe}_{1-x}\text{Mn}_x)\text{AsO}$ samples after Rietveld refinement in the $P4/nmm$ space group (synchrotron X-ray diffraction data).

		$\text{La}(\text{Fe}_{0.98}\text{Mn}_{0.02})\text{AsO}$			$\text{La}(\text{Fe}_{0.96}\text{Mn}_{0.04})\text{AsO}$		
Cell parameters	a (Å)	4.0372(1)			4.0391(1)		
	c (Å)	8.7505(1)			8.7640(1)		
Atomic site		x	y	z	x	y	z
La	$2c$	$\frac{1}{4}$	$\frac{1}{4}$	0.1411(1)	$\frac{1}{4}$	$\frac{1}{4}$	0.1409(1)
(Fe,Mn)	$2a$	$\frac{3}{4}$	$\frac{1}{4}$	$\frac{1}{2}$	$\frac{3}{4}$	$\frac{1}{4}$	$\frac{1}{2}$
As	$2c$	$\frac{1}{4}$	$\frac{1}{4}$	0.6518(1)	$\frac{1}{4}$	$\frac{1}{4}$	0.6521(1)
O	$2b$	$\frac{3}{4}$	$\frac{1}{4}$	0	$\frac{3}{4}$	$\frac{1}{4}$	0
R_F (%)		4.50			3.38		
R_{Bragg} (%)		8.75			2.97		

Table S2: Structural data at 10 K obtained for $\text{La}(\text{Fe}_{1-x}\text{Mn}_x)\text{AsO}$ samples after Rietveld refinement in the $Cmme$ space group (synchrotron X-ray diffraction data).

		La(Fe _{0.98} Mn _{0.02})AsO			La(Fe _{0.96} Mn _{0.04})AsO		
Cell parameters	a (Å)	5.7066(1)			5.7066(1)		
	b (Å)	5.6911(1)			5.7066(1)		
	c (Å)	8.7206(1)			8.7310(1)		
Atomic site		x	y	z	x	y	z
La	4g	0	¼	0.1417(1)	0	¼	0.1415(1)
(Fe,Mn)	4b	¼	0	½	¼	0	½
As	4g	0	¼	0.6511(1)	0	¼	0.6514(1)
O	4a	¼	0	0	¼	0	0
R_F (%)		5.43			4.97		
R_{Bragg} (%)		4.73			4.90		

Generally speaking, the variation of the lattice parameters of incommensurately modulated structures may induce microstrain-like anisotropic line broadening in powder diffractions patterns [1]. In this context, Figure S1 shows the superposition of the Williamson-Hall plots obtained after Rietveld refinements of the data collected at 10 K and 290 K ($x = 0.02$); for a sake of clarity, data at 10 K are reported according to the tetragonal setting. It is evident that low temperature data are affected by a micro-strain like contribution to the line broadening. From these data it can be concluded that microstrain increases by almost 30% along $[00l]$ and $\langle h00 \rangle$, but the gain exceeds 50% along $\langle hh0 \rangle$, which represents the direction of the Fermi surface nesting wave vector.

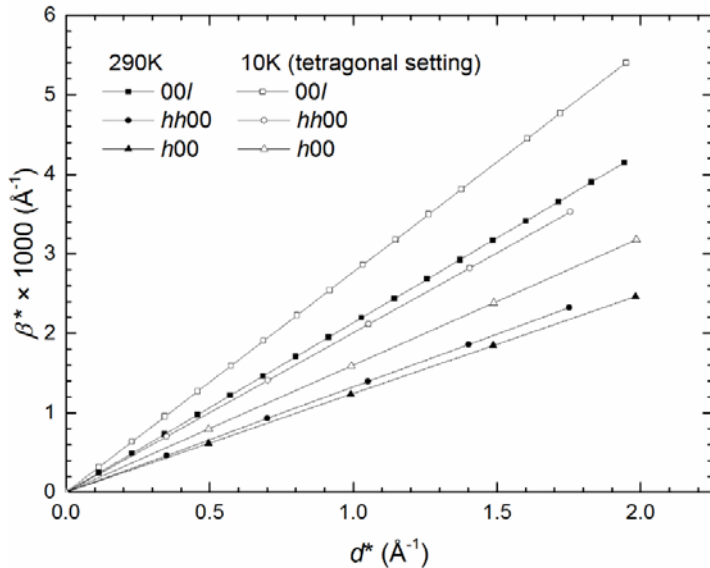


Figure S1: Superposition of the Williamson-Hall plots obtained after Rietveld refinements of the data collected at 10 K and 290 K for the La(Fe_{0.98}Mn_{0.02})AsO sample.

This behaviour complies with the case where only the parameters describing the average lattice vary in the different crystallites, but not the modulation vector¹. This is confirmed by the fact that the position of the satellite reflection remains constant with temperature.

S.2: Determination of the magnetic transition temperature

Neutron diffraction analysis is the best and direct probe of a magnetically ordered state. Preliminary data were collected for the $\text{La}(\text{Fe}_{0.98}\text{Mn}_{0.02})\text{AsO}$ sample using the high-intensity medium-resolution neutron powder D20 diffractometer of the Institute Laue-Langevin ($\lambda = 2.41 \text{ \AA}$). Remarkably, by these neutron diffraction data, also the structural transition temperature can be determined to $T_s = 113.5 \pm 0.5 \text{ K}$, in optimal agreement with the result obtained by synchrotron X-ray powder diffraction data. Figure S2 shows the thermal evolution of the magnetic moment as obtained after Rietveld refinement using the high-intensity neutron powder diffraction data; a $T_{\text{SDW}} = 99.5 \pm 0.5 \text{ K}$ results by fitting these data using a Landau mean field model $m(T) = m_0(1 - T/T_m)^\beta$, where m_0 is the magnetic moment extrapolated at $T = 0 \text{ K}$ and β is the critical exponent, which is $\frac{1}{2}$ in the case of pure 2nd order transitions. This result complies with the magnetization measurement; Figure S.3 shows the magnetization curve and the corresponding *erf* fit; the inflection point is located at $104.5 \pm 0.4 \text{ K}$, a few degrees above the long range AF order probed by neutrons.

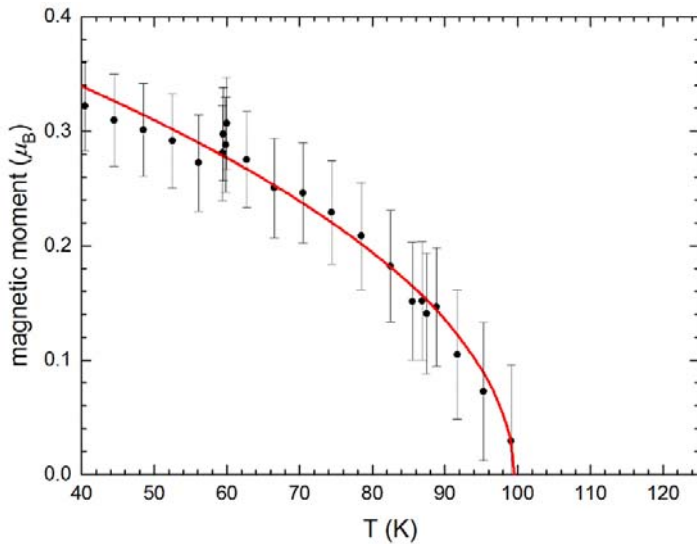


Figure S2: Thermal evolution of the magnetic moment in the $\text{La}(\text{Fe}_{0.98}\text{Mn}_{0.02})\text{AsO}$ sample as obtained after Rietveld refinement of high-intensity low-resolution neutron powder diffraction data; the data are fitted according to a Landau mean field theory valid for a 2nd order transition (red line).

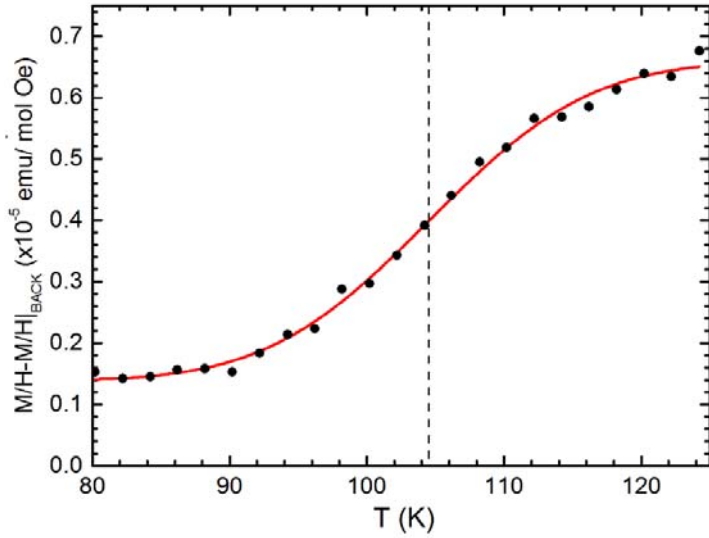


Figure S3: Temperature dependence of M/H measured under an applied field of 3 T in the magnetic transition region after subtracting a Curie–Weiss-like ‘background’ ($M/H|_{\text{BACK}}$) [2]; the red line represents the *erf*-fit whose inflection point is at $T \sim 104.5$ K (dashed line).

S.3: *dc* resistivity

Figure S4 shows the electrical resistivity (normalized to its value at $T = 300$ K) measured as a function of the temperature. The increase of the Mn content causes a suppression of structural/magnetic ordering temperature with a progressive smoothing of the typical step-like feature that characterizes the $x = 0$ composition around $T = 150$ K (blue curve in Figure S4). Moreover, the substitution of even a small amount of Mn substantially changes the nature of conduction. In fact in the $x = 0.01$ sample, the resistivity which decreases below the magnetic/structural transition, undergoes an abrupt upturn below 50 K. In the heavier substituted samples ($x = 0.02$ and 0.04) the low temperature upturn appears superimposed to a semiconducting-like behaviour starting at room temperature.

The inset of Figure S4 shows the evolution of the Hall coefficient curves, R_H vs T , as a function of the Mn content. The increase of the Mn content causes a suppression of the structural/magnetic ordering temperature and a progressive diminution of the absolute value, which can be ascribed to a compensation effect characteristic of a multiband system.

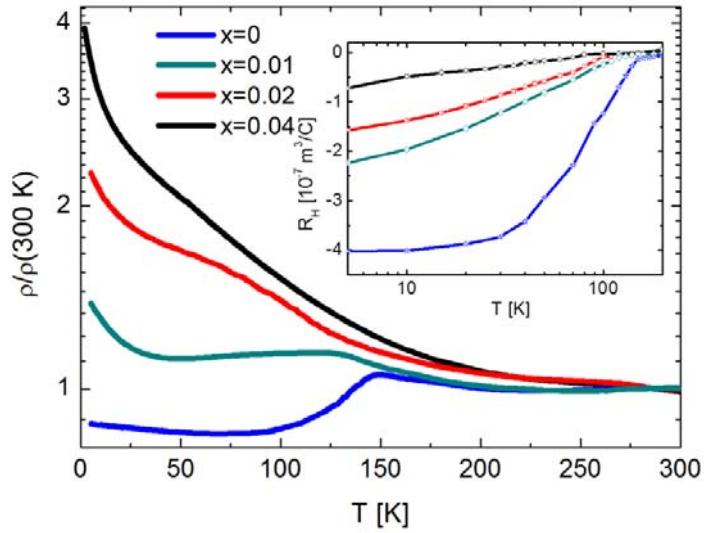


Figure S4: Normalized resistivity $\rho/\rho(300\text{ K})$ vs T measurement of $\text{La}(\text{Fe}_{1-x}\text{Mn}_x)\text{AsO}$ ($x = 0, 0.01, 0.02$ and 0.04) series; inset: Hall coefficient R_H vs T measurement of $\text{La}(\text{Fe}_{1-x}\text{Mn}_x)\text{AsO}$ ($x = 0, 0.01, 0.02$ and 0.04) series.

References

-
- [1] A. Leineweber, V. Petricek, Microstrain-like diffraction-line broadening as exhibited by incommensurate phases in powder diffraction patterns, *J. Appl. Cryst.* **40**, 1027 (2007)
- [2] McGuire, M. A., Hermann, R.P., Sefat, A. S., Sales, B.C., Jin, R., Mandrus, D., Grandjean, F., Long, G. J., *New J. Phys.* **11**, 025011 (2009)